

2D and 3D Modelling Strategies to Reproduce the Response of Historical Masonry Buildings Subjected to Settlements

Prosperi, Alfonso; Longo, Michele; Korswagen, Paul A.; Korff, Mandy; Rots, Jan G.

DOI

[10.1080/15583058.2024.2325472](https://doi.org/10.1080/15583058.2024.2325472)

Publication date

2024

Document Version

Final published version

Published in

International Journal of Architectural Heritage

Citation (APA)

Prosperi, A., Longo, M., Korswagen, P. A., Korff, M., & Rots, J. G. (2024). 2D and 3D Modelling Strategies to Reproduce the Response of Historical Masonry Buildings Subjected to Settlements. *International Journal of Architectural Heritage*, 19(5), 753-769. <https://doi.org/10.1080/15583058.2024.2325472>

Important note

To cite this publication, please use the final published version (if applicable).
Please check the document version above.

Copyright

Other than for strictly personal use, it is not permitted to download, forward or distribute the text or part of it, without the consent of the author(s) and/or copyright holder(s), unless the work is under an open content license such as Creative Commons.

Takedown policy

Please contact us and provide details if you believe this document breaches copyrights.
We will remove access to the work immediately and investigate your claim.

2D and 3D Modelling Strategies to Reproduce the Response of Historical Masonry Buildings Subjected to Settlements

Alfonso Prosperi, Michele Longo, Paul A. Korswagen, Mandy Korff & Jan G. Rots

To cite this article: Alfonso Prosperi, Michele Longo, Paul A. Korswagen, Mandy Korff & Jan G. Rots (06 Mar 2024): 2D and 3D Modelling Strategies to Reproduce the Response of Historical Masonry Buildings Subjected to Settlements, International Journal of Architectural Heritage, DOI: [10.1080/15583058.2024.2325472](https://doi.org/10.1080/15583058.2024.2325472)

To link to this article: <https://doi.org/10.1080/15583058.2024.2325472>



© 2024 The Author(s). Published with license by Taylor & Francis Group, LLC.



Published online: 06 Mar 2024.



Submit your article to this journal [↗](#)



Article views: 153



View related articles [↗](#)



View Crossmark data [↗](#)

2D and 3D Modelling Strategies to Reproduce the Response of Historical Masonry Buildings Subjected to Settlements

Alfonso Proserpi^a, Michele Longo^a, Paul A. Korswagen^a, Mandy Korff^{a,b}, and Jan G. Rots^a

^aFaculty of Civil Engineering and Geosciences, Delft University of Technology, Delft, The Netherlands; ^bGeoscience & Engineering, Technische Universiteit Delft, Delft, Netherlands

ABSTRACT

In this study, 2D and 3D modelling strategies are used to represent the behaviour of historical masonry buildings on strip foundations undergoing settlements. The application focuses on a two-story building, typical of the Dutch architectural heritage. An improved 2D modelling is presented: It includes the effect of the lateral walls to replicate the response of the detailed 3D models. The masonry strip foundation is modelled and supported by a no-tension interface, which represents the soil-foundation interaction. Two settlement configurations, hogging and sagging, are applied to the models, and their intensity is characterized using their angular distortion. The improved 2D model that includes the stiffness and weight of the lateral walls agrees in terms of displacements, stress and damage with the detailed 3D models. Conversely, the simplified 2D façade models without lateral walls exhibit different cracking, and damage from 2 to 7 times lower at an applied angular distortion of 2‰ (1/500). The improved 2D model requires less computational and modelling burden, resulting in analyses from 9 to 40 times faster than the 3D models. The results prove the importance of identifying and including the 3D effects that affect the response of structures subjected to settlements.

ARTICLE HISTORY

Received 14 December 2023
Accepted 24 February 2024

KEYWORDS

damage; masonry structures;
numerical modelling;
settlements

1. Introduction

Subsidence processes, induced by human activities and natural drivers, can lead to the settlement at the scale of single structures. In consequence, subsidence-induced settlements can harm existing historical masonry structures. This is the case in the western part of the Netherlands, in which the ubiquitous masonry structures rest on the subsurface prevalently made of highly compressible strata that enhance the settlement occurrence (Korswagen et al. 2023; Peduto et al. 2019; Proserpi et al. 2023b).

Settlement directly impacts historical structures supported by strip foundations, leading to deformation and damage. However, measurements of the deformation and damage of existing structures are often limited or unavailable. Thus, the accurate assessment of the response of the structure, which could serve as the basis for prediction models, poses a challenge.

The deformation and damage to the structure are often investigated via detailed numerical analyses. Both two- or more complex three-dimensional modelling approaches can be used to study the structural behaviour. However, it is crucial to correctly identify and

model the structural features that affect the response of the structure due to settlements, such as the effects of the lateral walls, i.e., the walls transversally connected to the façade, the floor and roof systems, and the foundation.

Additional uncertainties arise from the prediction and assessment of settlements affecting buildings: many natural or human subsidence drivers, such as the construction of new structures, changes in groundwater level and the oxidation of organic soils, can contribute to the overall subsidence and unpredictable ground profiles can arise (Charles and Skinner 2004; Drougkas, Verstryngge, Van Balen et al. 2020).

Both conventional and innovative techniques can be used to retrieve the deformation patterns of buildings (Peduto et al. 2019). For instance, air- or space-borne methods can be used to measure and monitor the displacement rates on structures (Peduto et al. 2017), providing a temporal depiction of building deformation. However, data acquired through air- or space-borne techniques may be limited by the temporal and/or spatial coverage, and require significant efforts in the processing and interpretation compared to conventional techniques.

Among conventional in-situ measurement techniques, the loss of horizontality of the bed joints can be measured to retrieve the deformation patterns of structures. However, for some walls of the structure, such as side walls shared among terraced houses, such measurements cannot be retrieved. In the case of masonry terraced buildings in the Netherlands, bed-joint measurements can only be retrieved along the front and/or façades. Consequently, the (numerical) analyses focus on the façade response as an alternative to evaluating the building's behaviour.

In this context, evaluating the best modelling strategies represents therefore a key task. In this study, the results of six 2D and 3D modelling strategies, selected from the state-of-the-art, are compared to identify the most suitable and less cost-effective model(s) in terms of modelling and computational burden. Among the selected models, an improved 2D model, originally proposed in (Prosperi et al. 2023a), includes the effects of the lateral walls in terms of stiffness and weight on the masonry building's response.

The aim is to provide background knowledge on the most suitable modelling techniques for masonry buildings undergoing ground settlement, with a focus on Dutch historical structures and their features.

This paper begins with a review of the underlying concepts in Section 2. In Section 3, the methodology is introduced, while in Section 4 the Finite Element Models are presented. The results are presented in Section 5. In Section 6, the conclusions are gathered.

2. Underlying concepts

2.1. Historical masonry buildings in the Netherlands

In the Netherlands, masonry is the predominant construction material, widely used for bridges, quay walls, windmills, water towers, and housing (Korswagen et al. 2023; Oktiovan, Messali, and Rots 2023; Sharma, Longo, and Messali 2023). In the west of the Netherlands, structures typically rest on strata of peat and clay highly predisposed to settle (Costa, Kok, and Korff 2020; Peduto et al. 2022). Although timber (and later concrete) piles, deeply driven into more stable soil, have been used for centuries (Klaassen 2008), strip foundations were adopted until 1925, with some examples dating back to the 1970s (Korswagen et al. 2023). Consequently, many historical masonry buildings rest on shallow foundations, which are directly exposed to the differential settlements (Costa, Kok, and Korff 2020).

Regarding the features of Dutch masonry houses, baked clay bricks dominate their masonry veneers (Jafari 2021). These houses are distinguishable for slender façades with large openings, connected at the corners with long transversal walls (Fusco et al. 2021; Grant et al. 2021). Examples of such buildings are shown in Figure 1. Moreover, masonry buildings built before World War II typically have timber floors and roofs (Francesco et al. 2018).

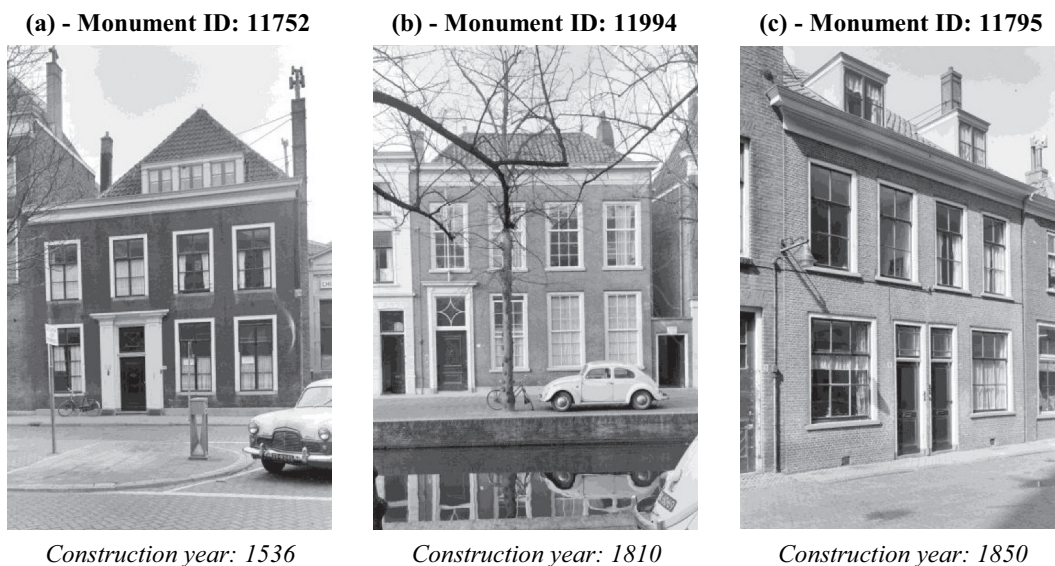


Figure 1. Examples of historical masonry buildings located in Delft, the Netherlands (Dukker 1964a, 1964b, 1964c). The information on the construction year was integrated from: bagviewer.Kadaster.nl.

2.2. Finite element analyses

Numerical analyses are often adopted to investigate the behaviour of structures subjected to different types of actions. Such numerical simulations should be always calibrated and validated against empirical observations. In some cases, however, the empirical knowledge and the in-situ measurements are limited or unavailable, and numerical models provide an alternative to investigate and predict the structure's response.

The accurate representation of the building, its features and the soil-structure interaction aims to correctly investigate the building's behaviour. Thus, it is critical to correctly model, both in the 2D and 3D analyses, the relevant building features that influence its response.

The advent of more high-performance computational resources has enabled the simulation of complex structural behaviour and the interaction with the soil to be more detailed and accurate (Giardina et al. 2013). The models of the structure subjected to settlement improved from equivalent approaches, such as linear-elastic beams with equivalent axial and bending stiffness, to more complex and detailed 2D and 3D models, which do not only include the non-linear behaviour of the materials, that are also able to investigate the induced cracking (Burd et al. 2000; Ferlisi et al. 2020; Ferlisi, Nicodemo, and Peduto 2019; Giardina et al. 2013; Netzel 2009; Netzel and Kaalberg 2000; Potts and Addenbrooke 1997; Rots 2001; Rots, Korswagen, and Longo 2021; Son and Cording 2005, 2007; Yiu, Burd, and Martin 2017).

In some modelling approaches, i.e., coupled analyses, the soil and the soil-structure interaction are included in the models. Whereas previous studies, included the soil as an elastic mass, the current approaches include its non-linear behaviour to accurately predict the settlements and the interaction with the structure (Franzius 2004; Giardina et al. 2013; Peduto et al. 2022; Potts and Addenbrooke 1997).

However, detailed and complex analyses, such as the above-mentioned coupled models, require the generation of complex meshes that, in turn, require high computational efforts (Giardina et al., 2013).

Therefore, an alternative is represented by semi-coupled models, in which the response of the structure is evaluated without the inclusion of the soil in the model.

In semi-coupled models, the ground settlements are imposed at the base of an interface that represents the foundation and the soil-structure interaction (Burd et al. 2022; Giardina et al. 2013; Rots 2001).

In some recent studies, the settlement is applied to an interface accounting for the soil-foundation interaction, while the strip foundation system is included in the

model (Giardina et al. 2013; Longo et al. 2021; Prospero et al. 2023a, 2023b; Rots, Korswagen, and Longo 2021); this is also the strategy employed in this paper and presented next.

3. Methodology

The adopted approach consists of three steps:

- In Step 0, the 2D and 3D modelling approaches for masonry structures subjected to ground settlements available in the state-of-the-art were reviewed.
- Based on this desk study, six modelling approaches were selected and used in Step 1 to generate the 2D and 3D numerical models for a two-story building on masonry strip foundations.
- The results of the numerical analyses were compared in Step 2 to investigate their differences. Thus, models are compared in terms of displacements, damage and stresses. Among the selected modelling strategies, the most efficient is selected as the one associated with the lowest computational burden and costs.

4. Finite element models

4.1. Modelling strategies

Six modelling approaches were selected from the literature. The models are herein built with the finite element software Diana FEA 10.5 to analyse a masonry building undergoing settlements. The selected strategies include 2D plane-stress analyses and 3D models. A schematic illustration of the six selected models and their features is shown in Figure 2, and are herein labelled as:

- (1) *2D Façade model (2DFA in Figure 2(a))*, a **plane-stress** two-dimensional model of the building's façade (Giardina et al. 2013; Bejarano-Urrego et al. 2019; Drougkas, Verstryngge, Szeker et al. 2020);
- (2) *2D façade model with Short Flanges (2DSF in Figure 2(b))*, a **plane-stress** two-dimensional model with one-brick lateral flanges, (i.e, 100 mm in the plane of the façade and 210 mm in the direction of the transverse walls) modelled with beam elements, that simulates the presence of lateral walls (Korswagen et al. 2019b; Rots, Korswagen, and Longo 2021; Prospero et al. 2023b);
- (3) *2D façade model with Long Flanges (2DLF in Figure 2(c))*, an improved **plane-stress** two-dimensional model with lateral flanges whose

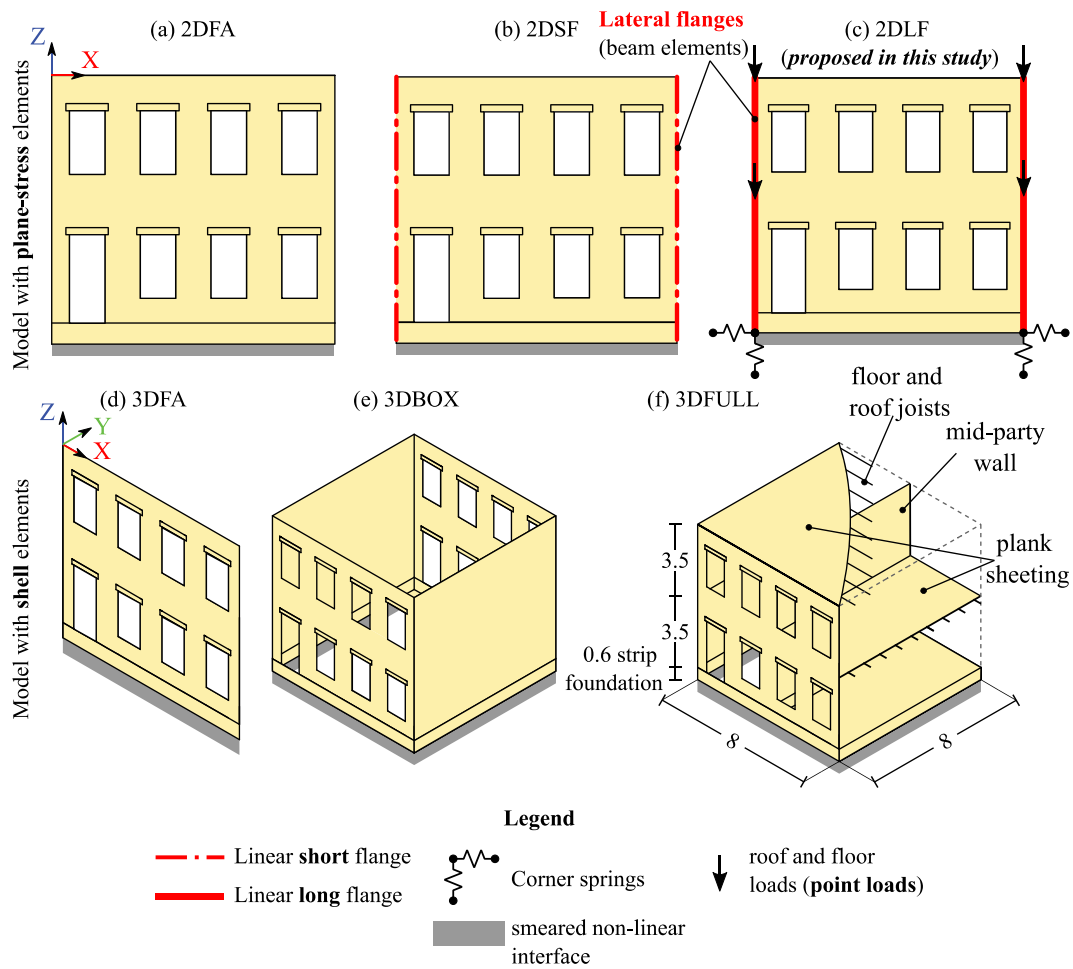


Figure 2. The six modelling approaches selected from the state-of-the-art: (a) 2D FAçade model (2DFA); (b) 2D façade with lateral short flanges (2DSF); (c) 2D façade with lateral long flanges (2DLF); (d) 3D FAçade model (3DFA); (e) 3D BOX model (3DBOX); (f) 3D FULL model (3DFULL). Measures in meters.

width is wider than one brick (i.e., higher than 210 mm in the direction of the transverse walls). The overburden given by the floor and roof are also included, differently from 2DFA and 2DSF (Prosperi et al. 2023a);

- (4) *3D FAçade model (3DFA in Figure 2(d))*, a *shell-elements* three-dimensional model of the building's façade; This model does not differ significantly from 2DFA, and it is included to check whenever differences can be observed using shell-elements rather than plane stress elements.
- (5) *3D BOX model (3DBOX in Figure 2(e))*, a *shell-elements* three-dimensional model of the entire building, without floors and party walls, similar to (Burd et al. 2000; Netzel and Kaalberg 2000; Giardina, Rots, and Hendriks 2013; Burd et al. 2022);
- (6) *3D FULL model (3DFULL in Figure 2(f))*, a *shell-elements* three-dimensional model of the entire building including a timber floor, timber roof

and an inner structural wall, similar to (Netzel and Kaalberg 2000; Yiu, Burd, and Martin 2017; Ferlisi, Nicodemo, and Peduto 2019; Giardina, Rots, and Hendriks 2013).

4.2. Geometry

The selected modelling strategies are employed to investigate the behaviour of a two-story masonry building. The façade of the selected building has a width of 8 meters (direction "X" in Figure 2), and a height of 7 meters. The selected building idealizes typical old Dutch houses (Jafari 2021), similar to the examples shown in Figure 1. Moreover, the façade represents a single-wythe wall (i.e. the width of one brick, equal to 100 mm, in direction "Y" in Figure 2) (Prosperi et al. 2023b). The lateral walls of the building have the same dimension and cross-section as the façade (Figure 1). Below each wall, the unreinforced masonry strip foundations are modelled. Such foundation typology is

commonly observed in such old Dutch buildings. The foundation is characterized by a base (perpendicularly to the façade, direction “Y” in Figure 2) equals to 500 mm and a height of 600 mm. In all the models, the façade include openings underneath masonry lintels.

4.3. FEM discretization

Regarding the mesh of the selected models, 8-node quadratic elements with 3×3 Gaussian integration schemes were adopted for the façade, lintels, and foundation for both the 2D and 3D analyses. A mesh size of 100×100 mm was used for the plane stress and curved shell elements, and 100 mm for the beam elements.

In the case of 3DFULL, the timber floor and timber roof, commonly observed in the Dutch historical buildings (Section 2.1), were modelled using the class-III Mindlin beam elements, representing the joists. Moreover, orthotropic shell elements were used for the plank sheeting. The floor, roof and mid-party wall were assumed to be disconnected from the front and back façades and to transmit the load to the transversal walls.

Similarly, in the case of the 2DSF and 2DLF models (Figure 2(b,c) respectively) Class-III Mindlin beam elements (DIANA 2021) were placed at the sides of the façade to model the effect of the transverse walls, following the approach implemented in (Korswagen et al. 2019b; Rots, Korswagen, and Longo 2021).

4.4. The effect of the lateral walls

The lateral elements simulate the additional stiffness and weight due to the presence of lateral walls and prevent the rotation of the façade’s edges (Korswagen et al. 2019b; Prospero et al. 2023b). The inclusion of lateral elements was observed to aid the development of realistic crack patterns due to ground settlements in similar studies (Korswagen et al. 2019b; Prospero et al. 2023b).

In the case of model 2DSF (Figure 2(b)), the presence of lateral walls is modelled with one-brick flanges (i.e., 100 mm in the plane of the façade and 210 mm in the direction of the transverse walls).

Regarding the improved 2D model, i.e., 2DLF (Figure 2(c)), an analytical approach is proposed to compute the length values (perpendicularly to the façade) adopted for lateral beam elements. This length corresponds to the “cooperating flange” of walls subjected to shear loading (NPR 2012-1-1:2012 nl 2012; Standard 2005); The cooperating flanges contribute added stiffness to the façade when it’s subjected to shear action, provided a good interlocking between the transverse and the façade (NPR 2012-1-1:2012 nl 2012; Standard 2005). In the case

of Dutch buildings (section 5.5.3 of NPR 2012-1-1:2012 nl 2012), the Dutch standard integrates this contribution with a normal compression force given by two areas. In these areas, the normal compressive force is provided by the part of the building wall located next to the cooperating flange width (from Standard 2005); this further contributes to the facade stability and stress redistribution in the case of shearing actions. In this study, the same value is used to describe the portion of the transverse walls that contribute to response of the façade subjected to settlements. Accordingly, the length of the cooperating flanges corresponds to the sum of three contributions (A1, A2a and A2b in Figure 3):

- The first contribution (A1 in Figure 3) was computed by considering the minimum of the following transverse wall properties: i) a fifth of the wall height ii) half of the internal distance between party walls ($L_s/2$) iii) six times the wall thickness (t), as described in (Standard 2005). The obtained value for the selected case is equal to 0.6 m;
- The second and the third contributions (A2a and A2b in Figure 3), correspond to the contribution to the normal compression given by the flange, as described in (NPR 2012-1-1:2012 nl 2012).

The sum of the three contributions (Flange thickness in Figure 3), i.e., the length of the flange for the model 2DLF is 2.35 m for the selected case;

Therefore, the computed value is about 11 times higher than the one used for the model with short flange 2DSF (which is equal to 210 mm), whereas the dimension is the same along the plane of the façade, i.e., 100 mm.

4.5. Material properties

The non-linear cracking behaviour of masonry behaviour of the masonry material was modelled employing an orthotropic, smeared crack/shear/crush constitutive law, i.e., the Engineering Masonry Model (Rots et al. 2016; Schreppers et al. 2016).

The parameters of the adopted constitutive law correspond to the material properties of the clay brick masonry (Table 1); Such material properties were retrieved from the Dutch Standard (NPR9998:2020en 2021) and previous studies (Korswagen et al. 2017; Schreppers et al. 2016). The Engineering Masonry Model was adopted for the façade, the lintels and the foundation.

The Young’s modulus equal to $1/3^{\text{rd}}$ of the one of the masonry material (E_y in Table 1) and a Poisson’s ratio equal to 0.15 were used for the lateral flanges in both the models 2DSF and 2DLF. The addition of lateral flanges

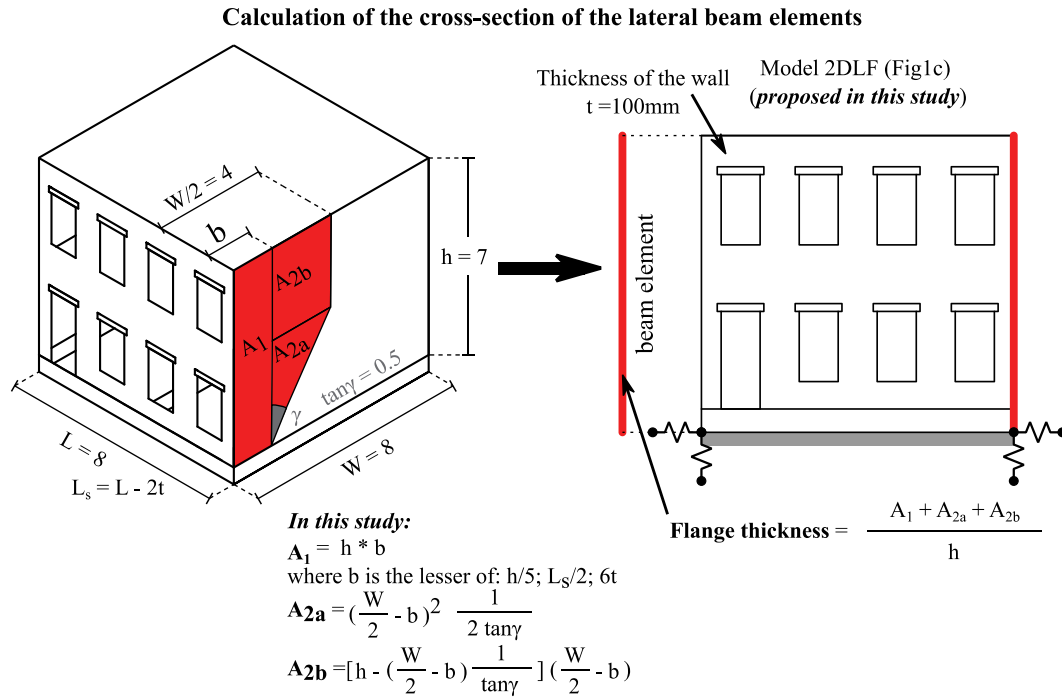


Figure 3. The calculation of the cross-section of the lateral beam elements used in the model 2DLF (Figure 2(c)). Measures in meters.

Table 1. Material properties adopted in the FE models.

Material properties	Symbol	Unit of measure	Value
Young's modulus vertical direction	E_y	[MPa]	5000
Young's modulus horizontal direction	E_x	[MPa]	2500
Shear modulus	G_{xy}	[MPa]	2000
Bed joint tensile strength	f_{ty}	[MPa]	0.10
Minimum head-joint strength	$f_{tx,min}$	[MPa]	0.15
Fracture energy in tension	$G_{ft,I}$	[N/mm]	0.01
Angle between stepped crack and bed-joint	α	[rad]	0.50
Compressive strength	f_c	[MPa]	8.50
Fracture energy in compression	G_c	[N/mm]	20.00
Friction angle	φ	[rad]	0.70
Cohesion	c	[MPa]	0.15
Fracture energy in shear	G_s	[N/mm]	0.10
Mass density	ρ	[Kg/m ³]	1708

with a reduced Young's modulus follows the calibration and validation presented in (Korswagen et al. 2019b); Accordingly, achieving realistic crack patterns was observed (Korswagen et al. 2019b; Rots, Korswagen, and Longo 2021).

The timber floor and timber roof are herein modelled using elastic C24 class (table 3.4 of (EN 2004-1-1 2004)) material for both the class-III Mindlin beam element and the orthotropic shell elements (DIANA 2021), calibrated according to the Appendix G of (NPR9998:2020en 2021).

The selected soil is characterized by the shear modulus equal to 10 MPa and the Poisson's ratio equal to 0.45. The soil material properties were adopted for the interface elements.

4.6. Interface elements

At the bottom edge of the strip foundation, a no-tension boundary interface was used to model the soil-foundation interaction (Longo et al. 2021). The interface has zero tensile strength, while it acts linearly in compression and shear. When an opening occurs, the shear stiffness is reduced to zero at that location.

In the case of both 2D and 3D models, six-noded line interface elements and the Newton-Cotes integration scheme are used (DIANA 2021). In particular, 2D models use 5 integration points, while for 3D models 3 integration points are used.

Interface elements require the definition of the normal (i.e., in the direction of gravity) and tangential (along the façade) stiffness. Such values are herein

computed using the analytical formulations reported by (Gazetas 1991; Mylonakis, Nikolaou, and Gazetas 2006; NEHRP 2012). The interface stiffnesses depend on soil shear modulus G , Poisson's ratio ν , and foundation base and length, following the approach implemented in (Prosperi et al. 2023b).

Additionally, the model 2DLF uses two corner springs below the transversal walls (Figure 2(c)) which are placed to support the additional weight of the lateral beam elements. The normal and tangential stiffness values computed for the interface elements are also assigned to the corner springs, by dividing the stiffness values by the area underneath the transversal wall.

4.7. Loadings

In all the selected models, settlements are modelled as displacements imposed at the base of the interface. This approach enables to fictitiously simulate the loss of support below the foundation due to the settlements, without having the soil unrealistically pull on the foundations (Prosperi et al. 2023b). The settlement actions idealize the occurrence of two types of asymmetric deformations (i.e. hogging and sagging in Figure 4) (Prosperi et al. 2023b). The imposed settlement deformations are based on field data and literature (Charles and Skinner 2004; Prospero et al., 2023b; Vent and Anne Elisabeth 2011). In the case of tunnelling-induced settlements, the ground movements are often observed to resemble Gaussian probability curves. However, in this work Gaussian curves are used also to idealize the deformations due to other sources of subsidence, similarly to Prospero et al., 2023b. The displacements imposed at the interface at the

base of the foundation were computed by means of Equation (1), adapted from Peck 1969:

$$S_v(x) = S_{v,max} e^{-\left(\frac{x-x_i}{2x_i}\right)^2} \quad (1)$$

Where $S_v(x)$ represents the vertical ground settlement at the location x ; x_i is the distance from the symmetric axis of the Gaussian curve to the point of inflection, and $S_{v,max}$ is a value that enables imposing the same intensity for all the profiles. In particular, the intensity of the settlement profiles is measured by the angular distortion β , i.e. the slope of the line joining two consecutive points in relation to a line joining the two points at the sides of each settlement profile (Burland and Wroth 1975); The angular distortion β is herein considered to be the maximum along the façade, following an approach implemented in (Prosperi et al. 2023b). Therefore, the $S_{v,max}$ is imposed so that the two settlement patterns are characterized by an angular distortion equal to $1/300$. Equation (1) allows the computation of two-dimensional curves; In the case of the 3D models, the settlement shapes obtained with Equation (1) are extruded in the direction perpendicular to the plane of the façade. This enables a consistent comparison between the results of all the models, as the façade is always subjected to the same imposed displacements. Therefore, the obtained settlement actions do not include the effects of three-dimensional settlement variations, which are explored for instance in (Zhao and DeJong 2023).

Moreover, in the model 3DFULL (Figure 2(f)) the effect of the overburden given by the timber floor and timber roof is included. In the case of the improved 2DLF model (Figure 2(c)), the overburden

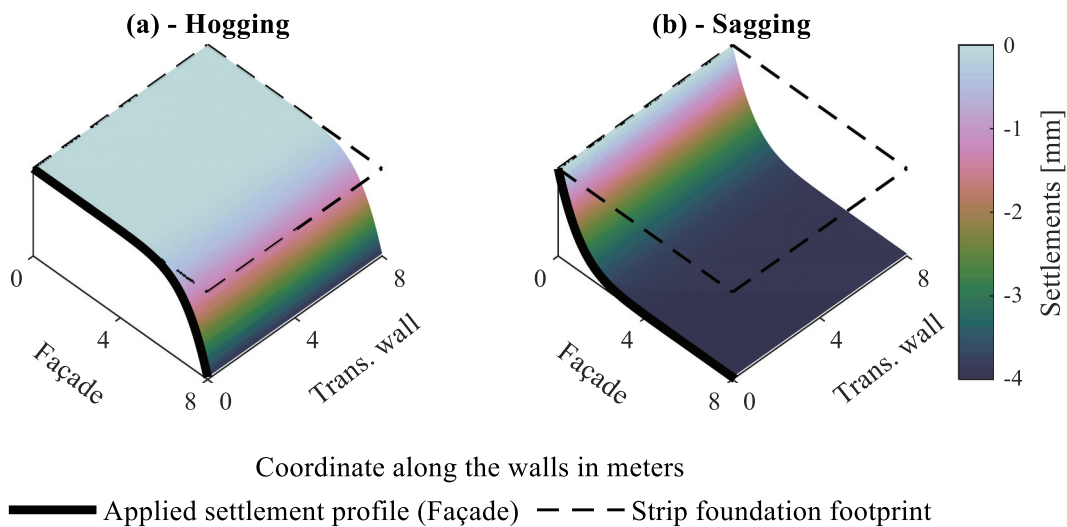


Figure 4. The two settlement shapes imposed at the base of the interfaces in the finite element models: (a) hogging and (b) sagging. The settlement profiles are conformed to a Gaussian curve. Their angular distortion is equal to $1/300$. Measures in meters.

of the floors was modelled by applying four equivalent point loads, two per floor at each side of the façade (Figure 2(c)); The intensity of the four equivalent point loads was computed considering the portion of the floor and roof that loads the length of the cooperating flanges.

The load application procedure includes two phases for all the selected models: First, the self-weight of the masonry structure, and eventually the overburden of the floors, was applied in 10 steps to obtain the initial stress-state. Then, the settlement is imposed at the base of the interface, and the intensity of the displacements is progressively increased in 195 steps (which correspond to a load rate of 0.02 mm/step).

4.8. Damage assessment

For each step of the numerical analyses, the tabulated output of the FEM models can be used to quantify the damage progression and accumulation. This is directly and objectively performed using the damage parameter Ψ , computed by means of Equation (2), proposed by (Korswagen et al. 2019), based on the number of cracks, their length and opening:

$$\Psi = 2n_c^{0.15} \hat{c}_w^{0.3} \quad (2)$$

Where n_c is the number of cracks, \hat{c}_w is the width-weighted and length averaged crack width (in mm) is computed with Equation (3):

$$\hat{c}_w = \frac{\sum_{i=1}^{n_c} c_{w,i}^2 c_{L,i}}{\sum_{i=1}^{n_c} c_{w,i} c_{L,i}} \quad (3)$$

Where $c_{w,i}$ is the maximum crack width along the i -crack in mm, while $c_{L,i}$ is the i -crack length in mm.

The values of Ψ provide objective estimates of the damage severity at each step of the analyses, which can be then categorized according to the system proposed by (Burland and Wroth 1975) (Table 2).

5. Results

5.1. Damage

An example of the progression of the damage for the model 2DLF (Figure 2(c)) and 3DFULL Figure 2(f) is shown in Figure 5.

For each model, the vertical displacements at the façade's base (top edge of the foundation) were retrieved. A distinction is therefore introduced between the applied deformations at the interface level, herein labelled as "applied", and the resulting façade displacements, identified as "retrieved" (Prosperi et al. 2023b). Thus, the angular distortion imposed at the interface level is labelled as " β_a ", whereas " β_r " is computed from the retrieved displacements.

Figure 6(a,b) show the relationship between the applied angular distortion β and the damage parameter Ψ .

It can be observed that the two façade models 2DFA (with plane stress elements) and 3DFA (with shell elements) show just minor differences (Figure 6). This observation confirms that no major differences can be attributed only to a change of the adopted finite elements (i.e. plane stress or shell elements). Moreover, the model 2DFA is associated with less computational and modelling burden than 3DFA.

The three-dimensional models, 3DBOX and 3DFULL, also show similar trends. Moreover, the more detailed 3D model exhibits higher damage for the same applied angular distortion, compared to the simplified façade models, 2DFA and 3DFA.

The results show how the model with a short lateral flange, 2DSF exhibits a trend comparable with the other simplified 2D analyses. Conversely, the proposed 2D model with a long lateral flange (i.e., 2DLF) shows a trend more similar to the more detailed 3D cases.

Interestingly, smaller differences between the trends of the models are observed when the retrieved angular distortion β_r is plotted against Ψ (Figure 6(c,f)); This observation proves that the retrieved deformation mainly depends on the shape and the stiffness of the façade itself. This is in agreement with the results of (Prosperi et al. 2023b). Regarding the ratio between the applied and the retrieved values of the angular

Table 2. Damage scale with the classification of visible damage and the corresponding discretization of the damage parameter Ψ (from (Burland, Baltzar Broms, and De Mello 1978; Grünthal 1998; Korswagen et al. 2019)).

Damage level	Degree of damage	Approximate crack width	Parameter of damage
DL0	No Damage	Imperceptible cracks	$\Psi < 1$
DL1	Negligible	up to 0.1 mm	$1 \leq \Psi < 1.5$
DL2	Very slight	up to 1 mm	$1.5 \leq \Psi < 2.5$
DL3	Slight	up to 5 mm	$2.5 \leq \Psi < 3.5$
DL4	Moderate	5 to 15 mm	$\Psi \geq 3.5$

An example of the Damage progression for Hogging

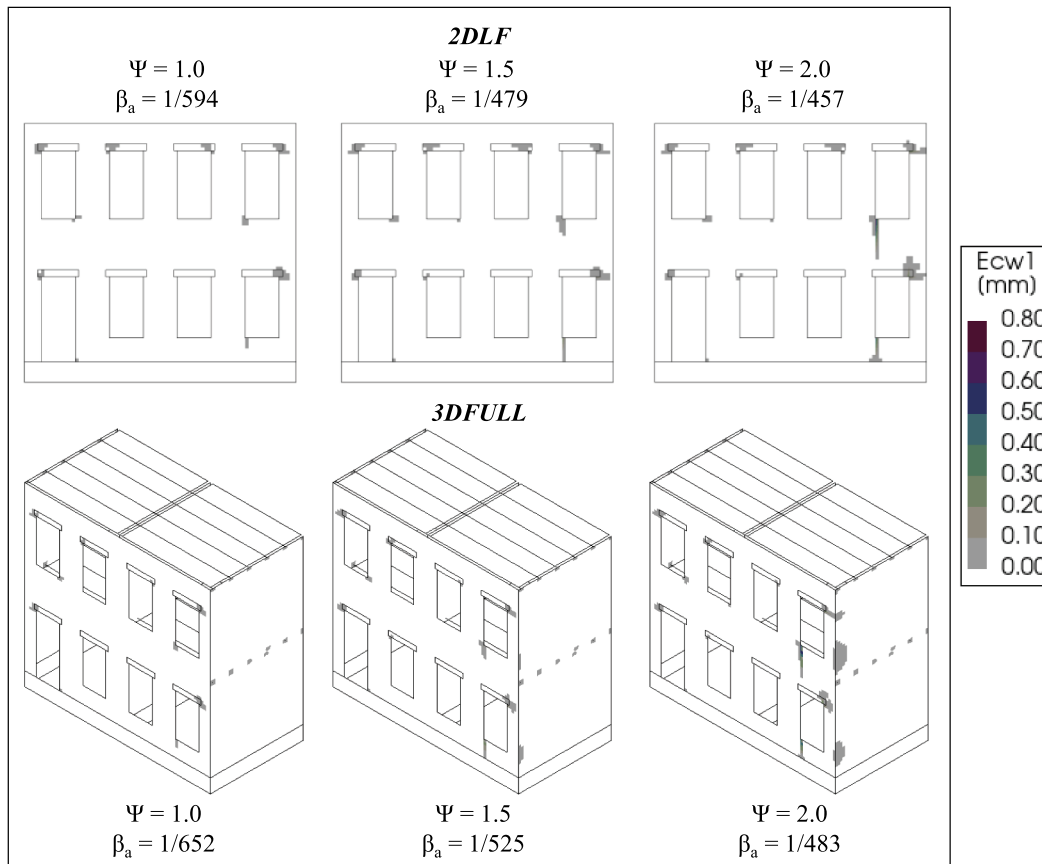


Figure 5. An example of the progression of the damage for model 2DLF (Figure 2(c)) and 3DFULL (Figure 2(f)) for the imposed hogging settlement (Figure 4(a)) for different values of imposed distortion β_a . The principal crack width (Ecw1) is shown. 3DFULL depicts half the model.

distortion, shown in Figure 6(e,f) for hogging and sagging respectively, the plotted lines are compared with a dash-dotted line that represents the condition for which applied and retrieved values would be equal (Figure 6).

The results of the models 2DLF, 3DBOX and 3DFULL progressively get closer to the theoretical line as the damage accumulates on the façade. Therefore, the 2DLF model better accommodates the imposed settlements with the damage progression. This behaviour is less clear for the model with short lateral elements, 2DSF. Conversely, the two simplified façade models, 2DFA and 3DFA, show a different trend.

For an applied angular distortion β_a equal to 2 ‰ (or 1/500), a comparison is shown in Figure 7 between the crack patterns (i.e. location and direction of the cracks) exhibited by all the models. For the selected angular distortion, the simplified façade models, 2DFA and 3DFA, and the model with short lateral elements, 2DSF, underestimate the damage (in terms of Ψ), both in hogging and sagging when compared with 3DFULL.

The 3DBOX model, in which the effects of the party wall and floors are not included, shows the highest damage in both hogging and sagging. The damage and crack patterns of the models 2DLF and 3DFULL are observed to be in good agreement.

5.2. Displacements

Figure 8 shows the comparison in terms of vertical (i.e., in the direction of gravity) displacements. The models, 2DFA, 3DFA and 2DSF exhibit different stiffer behaviour, i.e., less deformation, when compared to the models 2DLF, 3DBOX and 3DFULL in hogging and sagging (Figure 8). This is in agreement with the trends shown in Figure 6.

The inclusion of a flexible diaphragm in 3DFULL shows that the additional lateral confinement and extra overburden of the transversal walls do not influence the initiation and progression of the displacement-crack of the front facade. A small difference between 3DBOX and 3DFULL becomes visible when Ψ reaches a value of about 2.0. This confinement reduces the brittleness of the mechanism and

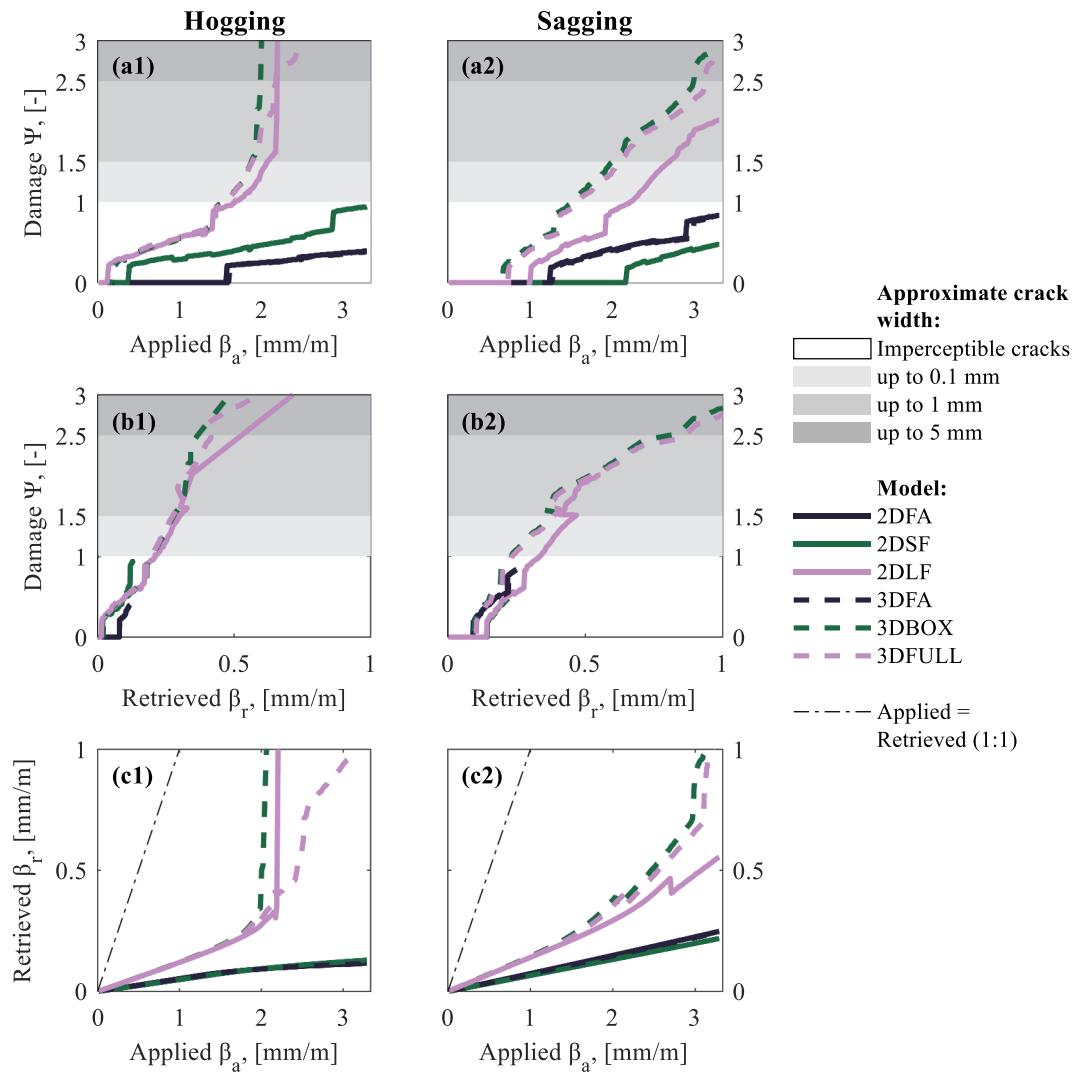


Figure 6. Applied and retrieved angular distortion β against the resulting damage parameter Ψ for all the FE models for both hogging and sagging. The results of the models 2DFA and 3DFA overlap in all the plots.

avoids larger out-of-plane displacement of the transversal walls. The confinement effect of the floor is mainly predominant when hogging deformation occurs (Figure 6).

Out-of-plane (OOP) displacements, i.e., perpendicular to the plane of the façade, are observable in the 3D models, differently from 2D ones, which do not include this feature. Figure 9 shows the out-of-plane displacements for the models 3DBOX and 3DFULL. Interestingly, the two models exhibit different OOP displacement patterns, both in hogging and sagging (Figure 9). For the selected value of angular distortion equal to 2 ‰ (or 1/500), the maximum absolute value of OOP displacement is equal to 0.25 millimetres.

5.3. Interface stresses

For the selected settlement intensity, i.e., β_a equal to 2 ‰ (or 1/500), a comparison between the normal

interface stresses is proposed in Figure 10. Accordingly, Figure 10 shows the results for both hogging and sagging. In both hogging and sagging, a good agreement is observed between the results of the models 2DLF, 3DBOX and 3DFULL. For instance, the stresses reveal that for the models 2DLF, 3DBOX and 3DFULL the entire interface is subjected to compression in the case of hogging. On the contrary, the models 2DFA, 2DSF and 3DFA show the formation of a gap at the right side of the façade, which means that that location reached zero compressive stress.

5.4. Features and performance of the models

The features of the numerical models in terms of type of elements, number of elements and nodes are shown in Table 3. Moreover, the CPU time of the analyses with the hogging (Figure 4(a)) settlement

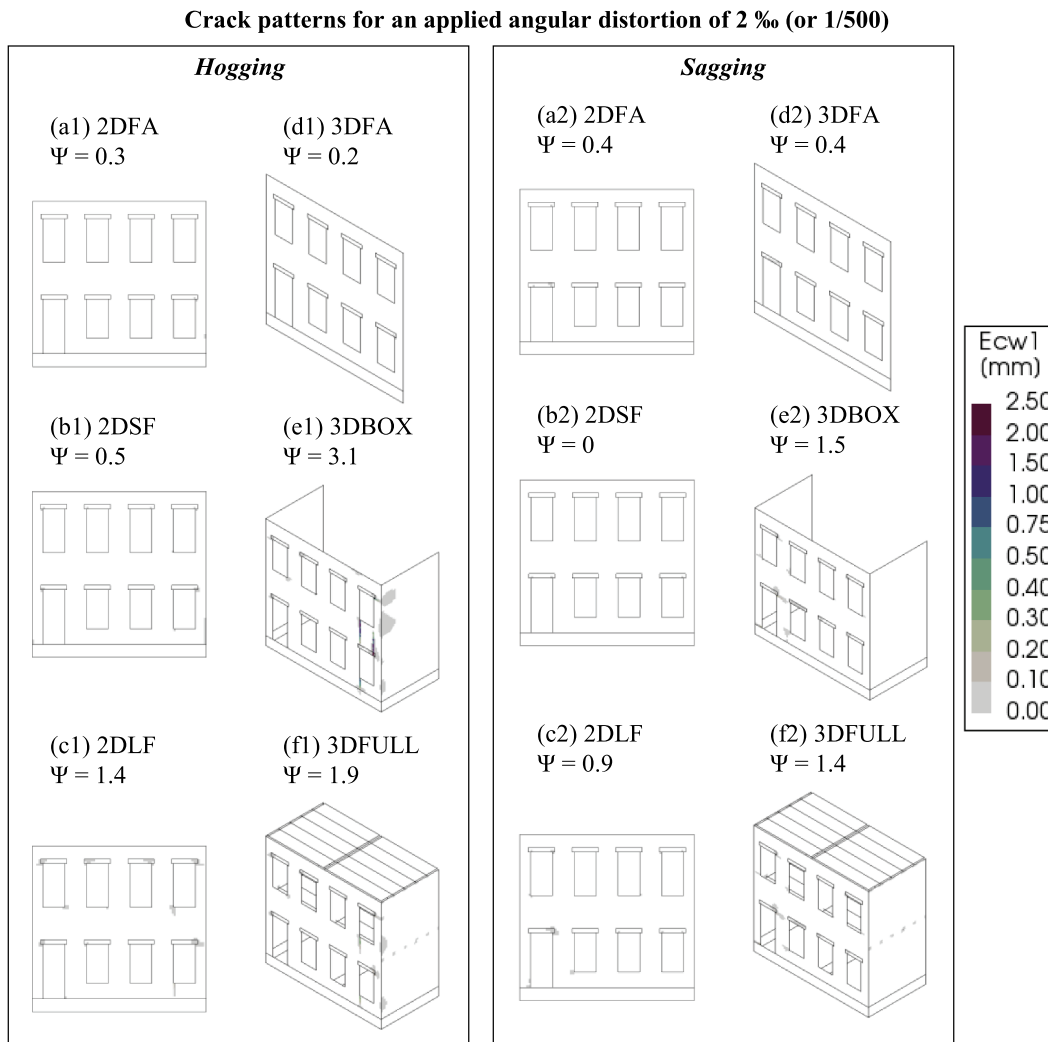


Figure 7. Resulting crack patterns for all the FE models at an applied angular distortion of 2 ‰ (or 1/500). The principal crack width (E_{cw1}) is shown. The damage parameter Ψ is reported for every model. (e1), (f1), (e2) and (f2) depict half the model.

action is reported. Additionally, as the 3D models can make use of the structural symmetry, two additional analyses that include this effect are included, and are herein labelled as 3DBOX-Half and 3DFULL-Half (Table 3). These estimates do not include the time to build the model, generate the mesh or set up the analyses. Moreover, the analysis time of each model was normalized to one of the proposed 2DLF model. The 2D models, 2DFA and 2DSF are the ones that require less computational time. The model 3DFA is 6 times slower than its plane-stress counterpart 2DFA. The models 3DBOX and 3DFULL are 37 to 40 times slower than the reference case, i.e., 2DLF; Even the models that make use of the structural symmetry, 3DBOX-Half and 3DFULL-Half, are 9 to 16 times slower than the reference case; Similar trends are observed in Sagging.

6. Discussion

In this study, different 2D and 3D modelling strategies, inspired by the state-of-the-art, for masonry buildings on strip foundations undergoing settlements are compared. The considered imposed loads are settlement deformations applied at the bottom of a boundary interface underneath the foundation. The imposed settlements do not present variations along the direction perpendicular to the plane of the façade. This assumption, however, serves the purpose of achieving a consistent comparison among the different modelling strategies. In the cases of structures undergoing settlements that highly resemble 3D patterns, 2D analyses may not be suitable to accurately depict the building response.

Regarding the imposed settlement, only the vertical components of the ground displacements are idealized

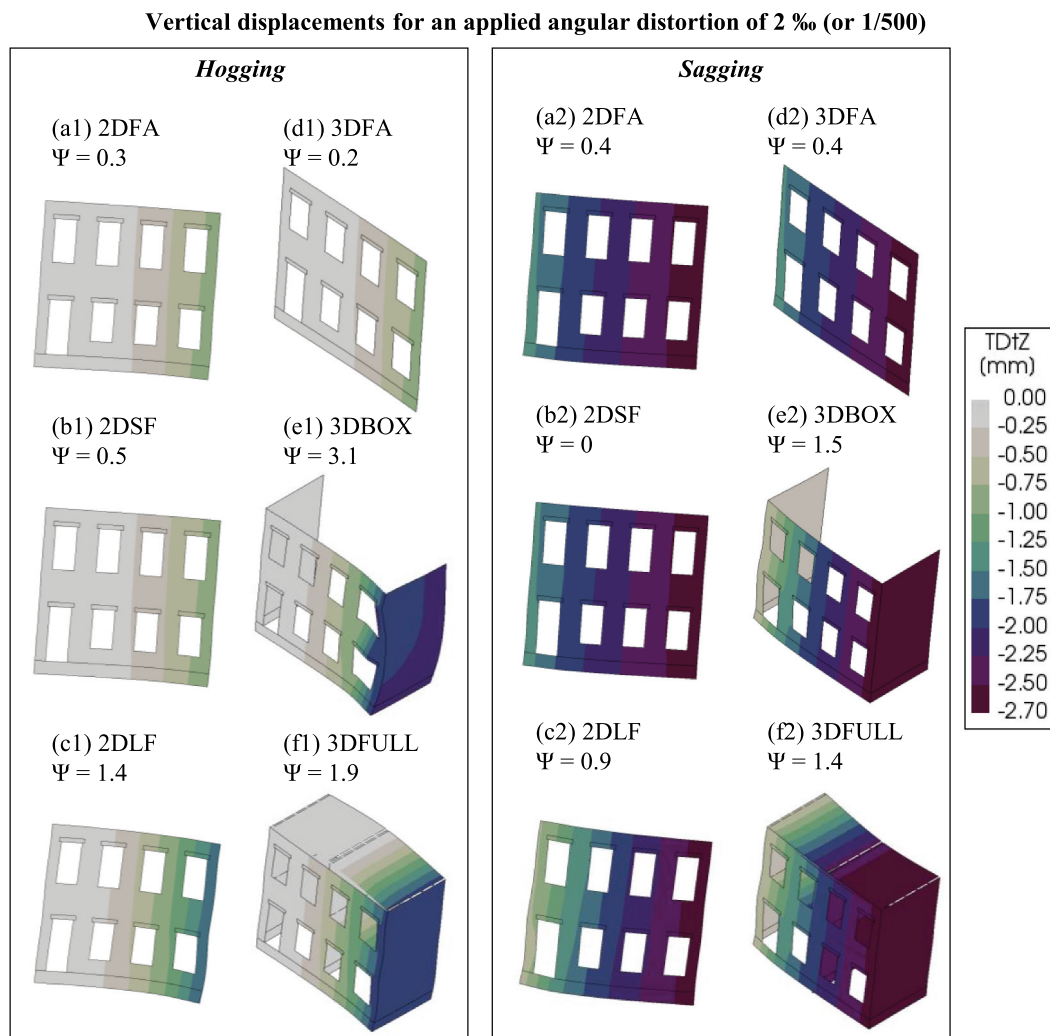


Figure 8. The resulting vertical displacements (TDtZ in the legend) for all the FE models at an applied angular distortion of 2 ‰ (or 1/500). Deformations are exaggerated (the magnification factor is equal to 500). The damage parameter Ψ is reported for every model. (e1), (f1), (e2) and (f2) depict half the model.

and considered. Conversely, the horizontal ground movements were purposely neglected. Horizontal ground movements play a key role in the case of settlement induced by human activities, such as tunnelling, mining or excavation works (Boscardin and Cording 1989); This study focuses instead on the effect of settlements that occur due to a combination of other subsidence sources (e.g. organic soil oxidation, groundwater lowering, soil shrinkage).

The soil deformations were herein imposed at the base of no-tension interfaces with a linear elastic behavior in shear. However, further analyses and future studies can benefit from the use of a soil friction angle to better simulate the contact at the base of the foundation, as shown in (Prosperi et al. 2023b).

Regarding the limitation of 2D modelling strategies, i.e., 2DFA, 2DSF and 2DLF, they are not able to include out-of-plane effects of the walls. In this study, out-of-

plane displacements in the 3DFA were not activated, while detailed 3D models, 3DBOX and 3DFULL reach a maximum of 1.7 mm at the end of the settlement applications, which is thus considered negligible. Previous studies, i.e. (Yiu, Burd, and Martin 2017, 2018), show that the difference between a 3D façade model, in which the 3D effects in terms of transverse wall and foundations are not included (similar to 3DFA) and a 3D full-structure model (similar to 3DBOX) provide similar results in terms of strains and damage for specific tunnelling-induced settlements; It should be noted, however, that the damage was there assessed considering the magnitude on the building maximum tensile strain, differently from this study. Additionally, such studies considered a different type of constitutive relation of the masonry material.

The results herein presented suggest that including the 3D effect of the lateral walls is crucial: the

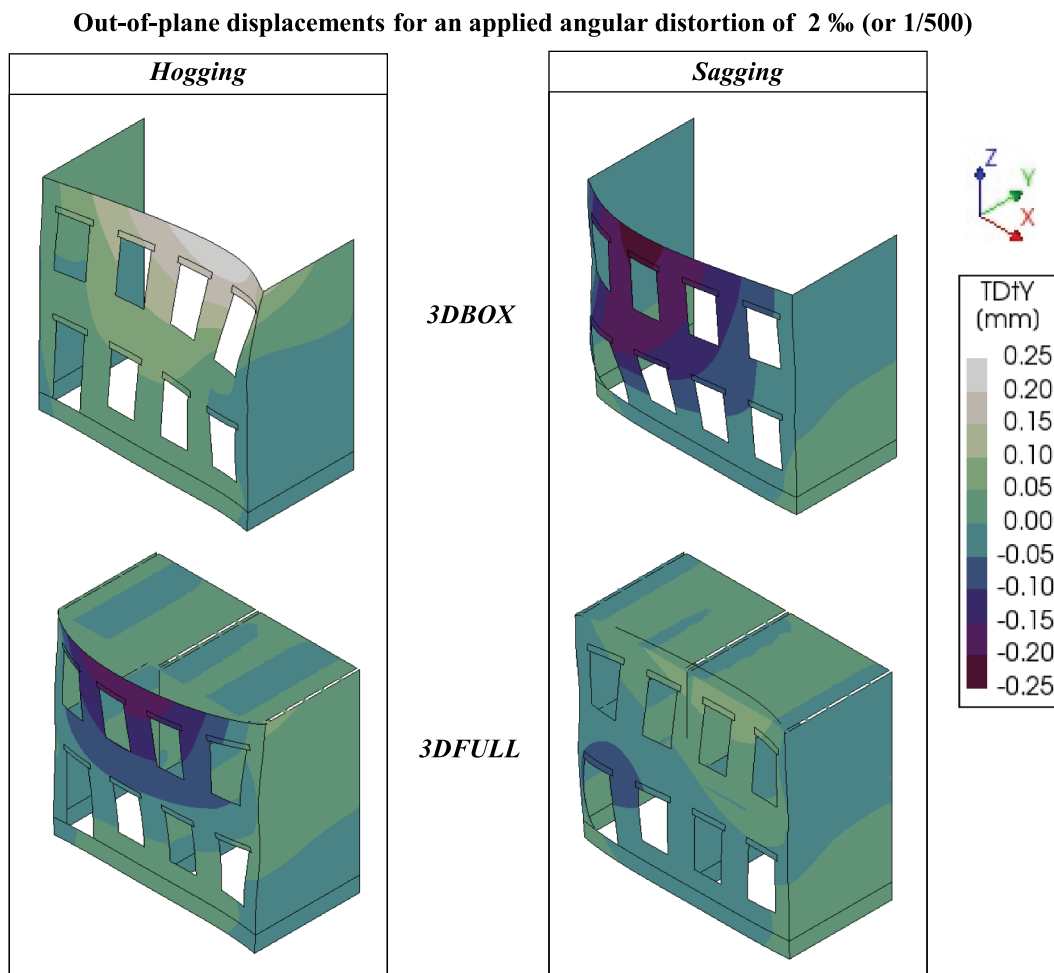


Figure 9. Out-of-plane (OOP) displacements (TDtY in the legend) for all the FE models 3DBOX and 3DFULL at an applied angular distortion of 2 ‰ (or 1/500) for both hogging and sagging. Deformations are shown and exaggerated along the direction of the transverse walls (the magnification factor is equal to 5000). The plots depict half the models.

interface stresses, displacements and cracking are all observed to be influenced by the weight and stiffness of lateral walls. The presence of a wider transversal wall (with additional weight) and the corner springs (additional stiffness) in the 2DLF model allows for a better representation of the three-dimensional effects. A similar effect at the side of the façades is expected when adjacent structures share transversal walls, in agreement with (Giardina, Rots, and Hendriks 2013).

The considered clay masonry façade and lateral walls idealize the structural inner leaves of old Dutch houses with cavity walls; Therefore both the façade and the lateral wall are characterized by the same wythe equal to 100 mm. However, it is expected that the results of this study can provide background to the analyses of cases characterized by the façade and the transverse walls with different wythes, such as for single wythe façade interlocked with double wythe house-to-house separation walls.

Additionally, although the use of linear elastic lateral elements in the model 2DSF and 2DLF serve as a modelling strategy rather than an actual depiction of the behaviour of the lateral walls, it was confirmed that the traction stresses to which they are subjected during the application of the settlement load never exceed the (bed joint) tensile strength of the masonry material; Consequently, the use linear-elastic elements were deemed suitable for the lateral walls in this study.

Further improvements of the proposed modelling approach may include the effect given by lateral walls with openings or the lateral confinement by the floor system; The inclusion of such effects can be attained, for instance, by means of discrete lateral springs. In this case, however, a 3DBOX model that does not include the timber floor and roof and the lateral walls only slightly differs in terms of deformation, crack pattern and stresses from the 3DFULL model in which such effects are included. This indicates that, for the reference case, the effects in terms of stiffness

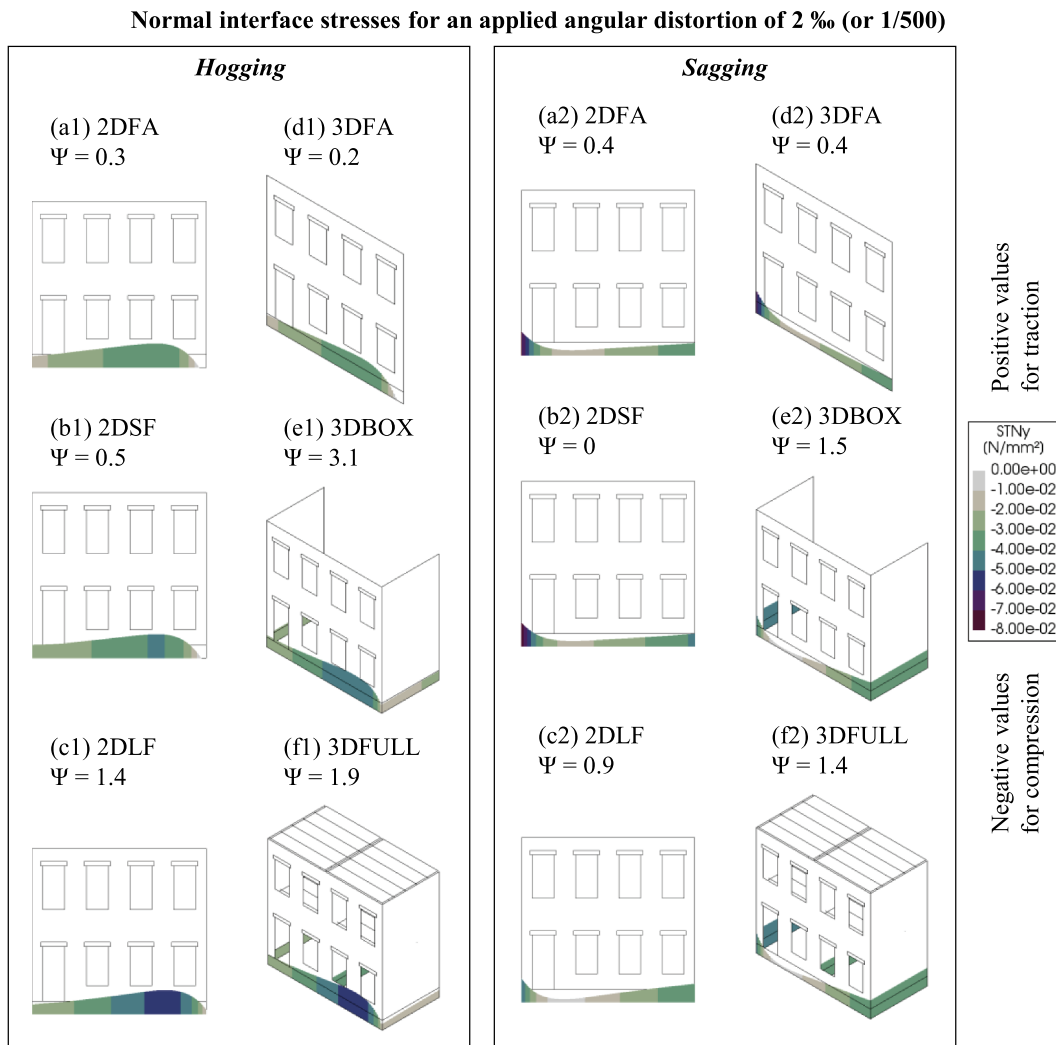


Figure 10. Normal (i.e., direction of gravity) interface stresses for hogging and sagging, with applied angular distortion of 2 ‰ (or 1/500). Positive values represent tension, and negative ones, compression. (e1), (f1), (e2) and (f2) depict half the model.

Table 3. A comparison of the performance of all the adopted models. The values of the proposed modelling approach 2DLF (Figure 2c) are shaded.

Model	Type of elements	Elements	Nodes	Analysis time [hh:mm:ss]	Normalized analysis time
2DFA	2D Plane Stress	4570	14414	00:08:41	0.36
2DSF	2D Plane Stress	4722	14414	00:08:25	0.35
2DLF	2D Plane Stress	4724	14414	00:24:18	1.00
3DFA	3D Shell	4650	14638	00:48:34	2.00
3DBOX	3D Shell	21620	66088	14:48:21	36.56
3DFULL	3D Shell	41580	121944	16:04:28	39.69
3DBOX-Half	3D Shell	10810	33198	03:50:18	9.48
3DFULL-Half	3D Shell	61436	20895	06:17:41	15.54

of the timber floor and roof system may be negligible. This is in agreement with the work of (Burd et al. 2000), in which it is reported that “*most of the mass and stiffness of a masonry building lies in the masonry itself*”.

7. Conclusion

The results of this study provide a background to the choice of the most suitable modelling strategy for masonry structures affected by ground movements. It was observed that:

- **It is key to pinpoint the structural features that affect the model response due to the settlement action:** the simplified façade of the building, 2DFA and 3DFA, that do not include the effects of the lateral walls, exhibit lower damage for a given applied angular distortion when compared with the more detailed three-dimensional models, 3DBOX and 3DFULL. For instance, for an applied angular distortion of 2 ‰ (or 1/500), the models that do not include the effect of the transverse walls, i.e., 2DFA and 3DFA exhibit a Ψ value from 2 to 7 times lower than the improved 2D modelling approach, labelled as 2DLF.
- The models without lateral walls exhibit lower vertical displacements than the models that include the effect of such walls. Therefore, **the response of the masonry façade is influenced not only by the stiffness but also by the weight of the lateral walls.**
- **The behaviour of all the considered models is influenced by the stress components developed at the interfaces. These stresses, in turn, are influenced by the inclusion of the weight of the lateral walls, which results in different stresses at the façade's edges.**
- The results of model 2D Long Flanges (2DLF), in terms of deformations, damage, displacements and interface stresses, are in good agreement with the ones of the more detailed 3D analyses. This observation suggests that **the improved 2D modelling strategy, 2D with lateral Long Flanges, depicts with good accuracy the behaviour of the entire structure subjected to settlement.**
- **The improved 2D modelling strategy, 2D with lateral Long Flanges, was observed to require less time and computational burden than the full-scale three-dimensional analyses.** The model 2DLF was observed to be from 9 to 40 times faster in terms of computational time than 3D analyses, due to a low model complexity.

Disclosure statement

No potential conflict of interest was reported by the author(s).

Funding

The research presented in this paper is part of the project Living on Soft Soils: Subsidence and Society (grantnr.: NWA.1160.18.259). This project is funded by the Dutch Research Council (NWO-NWA-ORC), Utrecht University, Wageningen University, Delft University of Technology,

Ministry of Infrastructure & Water Management, Ministry of the Interior & Kingdom Relations, Deltares, Wageningen Environmental Research, TNO-Geological Survey of The Netherlands, STOWA, Water Authority: Hoogheemraadschap de Stichtse Rijnlanden, Water Authority: Drents Overijsselse Delta, Province of Utrecht, Province of Zuid-Holland, Municipality of Gouda, Platform Soft Soil, Sweco, Tauw BV, NAM.

Credit authorship contribution statement

Alfonso Prospero: Conceptualization, Methodology, Software, Formal analysis, Investigation, Data curation and processing, Writing — review & editing. **Michele Longo:** Conceptualization, Methodology, Software, Formal analysis, Investigation, Data curation and processing, Writing — review & editing. **Paul A. Korswagen:** Conceptualization, Methodology, Software, Supervision, Writing — review & editing. **Mandy Korff:** Conceptualization, Supervision, Review, Funding acquisition. **Jan G. Rots:** Conceptualization, Supervision, Review, Funding acquisition.

References

- Bejarano-Urrego, L., E. Verstryngne, A. Drougkas, G. Giardina, M. Bassier, M. Vergauwen, and K. Van Balen. 2019. "Numerical analysis of settlement-induced damage to a masonry church nave wall." In *Structural analysis of historical constructions*, edited by R. Aguilar, D. Torrealva, S. Moreira, M. A. Pando, L. F. Ramos, 853–861. Cham: Springer International Publishing.
- Boscardin, M. D., and E. J. Cording. 1989. Building response to excavation-induced settlement. *Journal of Geotechnical Engineering-Asce* 115 (1):1–21. doi:10.1061/(Asce)0733-94101989).
- Burd, H. J., G. T. Houlsby, C. E. Augarde, and G. Liu. 2000. Modelling tunnelling-induced settlement of masonry buildings. *Proceedings of the Institution of Civil Engineers-Geotechnical Engineering* 143 (1):17–29. doi:10.1680/geng.2000.143.1.17.
- Burd, H. J., W. N. Yiu, S. Acikgoz, and C. M. Martin. 2022. Soil-foundation interaction model for the assessment of tunnelling-induced damage to masonry buildings. *Tunnelling and Underground Space Technology* 119:104208.
- Burland, J. B., B. Baltzar Broms, and V. F. De Mello. 1978. Behaviour of foundations and structures, IX ICSMFE, Tokyo, 1977.
- Burland, J. B., and C. P. Wroth. 1975. Settlement of buildings and associated damage.
- Charles, J. A., and H. D. Skinner. 2004. Settlement and tilt of low-rise buildings. *Proceedings of the Institution of Civil Engineers-Geotechnical Engineering* 157 (2):65–75. doi:10.1680/geng.2004.157.2.65.
- Costa, A. L., S. Kok, and M. Korff. 2020. Systematic assessment of damage to buildings due to groundwater lowering-induced subsidence: Methodology for large scale application in the Netherlands. *Proceedings of the International Association of Hydrological Sciences* 382:577–82. doi:10.5194/piahs-382-577-2020.

- DIANA, F. E. A. 2021. *Finite element analysis User's manual - release 10.5*. Delft, The Netherlands: DIANA FEA BV.
- Drougkas, A., E. Verstryngge, P. Szeker, G. Heirman, L. E. Bejarano-Urrego, G. Giardina, and K. Van Balen. 2020. Numerical modeling of a church nave wall subjected to differential settlements: Soil-structure interaction, time-dependence and sensitivity analysis. *International Journal of Architectural Heritage* 14 (8):1221–38. doi:10.1080/15583058.2019.1602682.
- Drougkas, A., E. Verstryngge, K. Van Balen, M. Shimoni, T. Croonenborghs, R. Hayen, and P. Y. Declercq. 2020. Country-scale InSAR monitoring for settlement and uplift damage calculation in architectural heritage structures. *Structural Health Monitoring-An International Journal* 1475921720942120. doi:10.1177/1475921720942120.
- Dukker, G. J. 1964a. Gevel - Delft - 20050796 - RCE.jpg. In, https://commons.wikimedia.org/wiki/File:Gevel_-_Delft_-_20050796_-_RCE.jpg. Rijksdienst voor het Cultureel Erfgoed, CC BY-SA 4.0. via Wikimedia Commons.
- Dukker, G. J. 1964b. Gevel - Delft - 20052535 - RCE.jpg. In, https://commons.wikimedia.org/wiki/File:Gevel_-_Delft_-_20052535_-_RCE.jpg. Rijksdienst voor het Cultureel Erfgoed, CC BY-SA 4.0. via Wikimedia Commons.
- Dukker, G. J. 1964c. Gevels - Delft - 20050939 - RCE.jpg. In, https://commons.wikimedia.org/wiki/File:Gevels_-_Delft_-_20050939_-_RCE.jpg. Rijksdienst voor het Cultureel Erfgoed, CC BY-SA 4.0. via Wikimedia Commons.
- EN 1995-1-1. 2004. *Eurocode 5: Design of timber structures - part 1-1: General - common rules and rules for buildings*. Brussels: CEN.
- Ferlisi, S., G. Nicodemo, and D. Peduto. 2019. Numerical analysis of the behaviour of masonry buildings undergoing differential settlements, **17th European Conference on Soil Mechanics and Geotechnical Engineering**, Reykjavik. London: **International Society for Soil Mechanics and Geotechnical Engineering (ISSMGE)**. doi:10.32075/17ECMGE-2019-0450.
- Ferlisi, S., G. Nicodemo, D. Peduto, C. Negulescu, and G. Grandjean. 2020. Deterministic and probabilistic analyses of the 3D response of masonry buildings to imposed settlement troughs. *Georisk-Assessment and Management of Risk for Engineered Systems and Geohazards* 14 (4):260–79. doi:10.1080/17499518.2019.1658880.
- Francesco, M., R. Esposito, G. R. Samira Jafari, P. Korswagen, and G. Rots. 2018. A multiscale experimental characterisation of Dutch unreinforced masonry buildings. Paper presented at the 16th European Conference on Earthquake Engineering, Thessaloniki. Springer.
- Franzius, J. N. 2004. *Behaviour of buildings due to tunnel induced subsidence*. Imperial College London (University of London).
- Fusco, D., FRANCESCO Messali, J. Rots, D. Addressi, and S. Pampanin. 2021. Numerical study of pier-wall connections in typical Dutch URM buildings. Paper presented at the 12th International Conference on Structural Analysis of Historical Constructions: SAHC 2021, Online event 29 Sep-1 Oct, Online.
- Gazetas, G. 1991. Foundation vibrations. In *Foundation engineering handbook*, 553–93. Boston, MA: Springer.
- Giardina, G., J. G. Rots, and M. A. N. Hendriks. 2013. Modelling of settlement induced building damage. Delft University of Technology.
- Giardina, G., A. V. Van de Graaf, M. A. N. Hendriks, J. G. Rots, and A. Marini. 2013. Numerical analysis of a masonry facade subject to tunnelling-induced settlements. *Engineering Structures* 54:234–47. doi:10.1016/j.engstruct.2013.03.055.
- Grant, D. N., J. Dennis, R. Sturt, G. Milan, D. McLennan, P. Negrette, R. da Costa, and M. Palmieri. 2021. Explicit modelling of collapse for Dutch unreinforced masonry building typology fragility functions. *Bulletin of Earthquake Engineering* 19 (15):6497–519.
- Grünthal G.1998. *European Macroseismic Scale 1998 EMS-98*. Luxembourg:European Seismological Commission.
- Jafari, S. 2021. Material characterisation of existing masonry: A strategy to determine strength, stiffness and toughness properties for structural analysis. *Delft University of Technology: TU Delft Applied Mechanics* [Https://Repository Tudelft Nl Doctoral Thesis](https://Repository.Tudelft.nl/DoctoralThesis). Delft University of Technology.
- Klaassen, R. K. W. M. 2008. Bacterial decay in wooden foundation piles-patterns and causes: A study of historical pile foundations in the Netherlands. *International Biodeterioration & Biodegradation* 61 (1):45–60. doi:10.1016/j.ibiod.2007.07.006.
- Korswagen, P. A., M. Longo, E. Meulman, and J. Rots. 2019b. Experimental and computational study of the influence of pre-damage patterns in unreinforced masonry crack propagation due to induced, repeated earthquakes. Paper presented at the 13th North American Masonry Conference, Salt Lake City, Utah.
- Korswagen, P. A., M. Longo, E. Meulman, and J. G. Rots. 2019a. Crack initiation and propagation in unreinforced masonry specimens subjected to repeated in-plane loading during light damage. *Bulletin of Earthquake Engineering* 17 (8):4651–87.
- Korswagen, P. A., M. Longo, E. Meulman, and C. A. van Hoogdalem. 2017. *Damage sensitivity of Groningen masonry structures – Experimental and computational studies*.
- Korswagen, P. A., M. Longo, A. Prospero, J. G. Rots, and K. C. Terwel. 2023. Modelling of damage in historical masonry façades subjected to a combination of ground settlement and vibrations. Paper presented at the International Conference on Structural Analysis of Historical Constructions, Kyoto, Japan.
- Longo, M., M. Sousamli, P. A. Korswagen, P. van Staalduinen, and J. G. Rots. 2021. Sub-structure-based ‘three-tiered’ finite element approach to soil-masonry-wall interaction for light seismic motion. *Engineering Structures* 245:112847. doi:10.1016/j.engstruct.2021.112847.
- Mylonakis, G., S. Nikolaou, and G. Gazetas. 2006. Footings under seismic loading: Analysis and design issues with emphasis on bridge foundations. *Soil Dynamics and Earthquake Engineering* 26 (9):824–53. doi:10.1016/j.soildyn.2005.12.005.
- NEHRP. 2012. *NIST GCR 12-917-21 soil-structure interaction for building structures*. Gaithersburg: National Institute of Standards and Technology, US Department of Commerce.
- Netzel, H. D. 2009. Building response due to ground movements.

- Netzel, H., and F. J. Kaalberg. 2000. Numerical damage risk assessment studies on adjacent buildings in Amsterdam. Paper presented at the ISRM International Symposium, Melbourne, Australia.
- NPR 9096-1-1:2012 nl. 2012. *Steenconstructies - Eenvoudige ontwerpregels, gebaseerd op NEN-EN 1996-1-1+C1 (Masonry structures - Simple design rules, based on NEN-EN 1996-1-1+C1)*.
- NPR9998:2020en. 2021. Assessment of structural safety of buildings in case of erection, reconstruction and disapproval – induced earthquakes – basis of design, actions and resistances.
- Oktiovan, Y. P., F. Messali, and J. Rots. 2023. Detailed distinct element modeling of a Utrecht wharf cellar for the assessment of the load-bearing capacity and failure mechanism. Paper presented at the Proceedings of the Seventeenth International Conference on Civil, Structural and Environmental Engineering Computing, Kyoto, Japan.
- Peck, R. B. 1969. Deep excavations and tunneling in soft ground. *Proceeding 7th ICSMFE* 1969:225–90.
- Peduto, D., M. Korff, G. Nicodemo, A. Marchese, and S. Ferlisi. 2019. Empirical fragility curves for settlement-affected buildings: Analysis of different intensity parameters for seven hundred masonry buildings in the Netherlands. *Soils & Foundations* 59 (2):380–97. doi:10.1016/j.sandf.2018.12.009.
- Peduto, D., G. Nicodemo, J. Maccabiani, and S. Ferlisi. 2017. Multi-scale analysis of settlement-induced building damage using damage surveys and DInSAR data: A case study in the Netherlands. *Engineering Geology* 218:117–33. doi:10.1016/j.enggeo.2016.12.018.
- Peduto, D., A. Prosperi, G. Nicodemo, and M. Korff. 2022. District-scale numerical analysis of settlements related to groundwater lowering in variable soil conditions. *Canadian Geotechnical Journal* 99 (999):1–16.
- Potts, D. M., and T. I. Addenbrooke. 1997. A structure's influence on tunnelling-induced ground movements. *Proceedings of the Institution of Civil Engineers-Geotechnical Engineering* 125 (2):109–25. doi:10.1680/igeng.1997.29233.
- Prosperi, A., M. Longo, P. A. Korswagen, M. Korff, and J. G. Rots. 2023a. Accurate and efficient 2D modelling of historical masonry buildings subjected to settlements in comparison to 3D approaches. Paper presented at the International Conference on Structural Analysis of Historical Constructions, Kyoto, Japan.
- Prosperi, A., M. Longo, P. A. Korswagen, M. Korff, and J. G. Rots. 2023b. Sensitivity modelling with objective damage assessment of unreinforced masonry façades undergoing different subsidence settlement patterns. *Engineering Structures* 286:116113.
- Rots, J. G. 2001. Computational modelling of cracking and settlement damage in masonry structures. Paper presented at the Proceeding 12th International Brick/Block Masonry Conference, Madrid, Spain.
- Rots, J. G., P. A. Korswagen, and M. Longo. 2021. *Computational modelling checks of masonry building damage due to deep subsidence*. The Netherlands: Delft University of Technology.
- Rots, J. G., F. Messali, R. Esposito, S. Jafari, and V. Mariani. 2016. Thematic keynote computational modelling of masonry with a view to Groningen induced seismicity. Paper presented at the Structural Analysis of Historical Constructions: Anamnesis, Diagnosis, Therapy, Controls: Proceedings of the 10th International Conference on Structural Analysis of Historical Constructions, SAHC, Leuven, Belgium, September 13–15.
- Schreppers, G. M. A., A. Garofano, F. Messali, and J. G. Rots. 2016. DIANA validation report for masonry modelling. *DIANA FEA report*.
- Sharma, S., M. Longo, and F. Messali. 2023. A novel tier-based numerical analysis procedure for the structural assessment of masonry quay walls under traffic loads. *Frontiers in Built Environment* 9:1194658.
- Son, M., and E. J. Cording. 2005. Estimation of building damage due to excavation-induced ground movements. *Journal of Geotechnical and Geoenvironmental Engineering* 131 (2):162–77. doi:10.1061/(Asce)1090-0241.
- Son, M., and E. J. Cording. 2007. Evaluation of building stiffness for building response analysis to excavation-induced ground movements. *Journal of Geotechnical and Geoenvironmental Engineering* 133 (8):995–1002. doi:10.1061/(Asce)1090-0241.
- Standard, B. 2005. Eurocode 6—design of masonry structures—. British Standard Institution: London.
- Vent, D., and I. Anne Elisabeth. 2011. Structural damage in masonry: Developing diagnostic decision support. Delft University of Technology.
- Yiu, W. N., H. J. Burd, and C. M. Martin. 2017. Finite-element modelling for the assessment of tunnel-induced damage to a masonry building. *Geotechnique* 67 (9):780–94.
- Yiu, W. N., H. J. Burd, and C. M. Martin. 2018. Soil-foundation contact models in finite element analysis of tunnelling-induced building damage. Paper presented at the Numerical Methods in Geotechnical Engineering IX, Volume 2: Proceedings of the 9th European Conference on Numerical Methods in Geotechnical Engineering (NUMGE 2018), Porto, Portugal, June 25–27, 2018.
- Zhao, J., and M. DeJong. 2023. Three-dimensional probabilistic assessment of tunneling induced structural damage using monte-carlo method and hybrid finite element model. *Computers and Geotechnics* 154:105122.